Sensors and Materials, Vol. 38, No. 2 (2026) 653–661
MYU Tokyo

S & M 4334

Development of Pr-doped $Gd_3Al_3Ga_2O_{12}$ Nanoparticles for *In vivo* Applications

Masanori Koshimizu,[1,2*] Kazuki Tanahashi,[2] Yutaka Fujimoto,[3] and Keisuke Asai[3]

[1]Research Institute of Electronics, Shizuoka University, 3-5-1 Johoku, Chuo-ku, Hamamatsu 432-8011, Japan
[2]Electronics and Materials Science Department, Faculty of Engineering, Shizuoka University, 3-5-1 Johoku, Chuo-ku, Hamamatsu 432-8011, Japan
[3]Department of Applied Chemistry, Graduate School of Engineering, Tohoku University, 6-6-07 Aoba, Aramaki, Aoba-ku, Sendai 980-8579, Japan

(Received October 25, 2025; accepted December 10, 2025)

Keywords: scintillator, nanoparticle, garnet, *in viv*o, Pr^{3+}

Nanoparticle scintillators have been used in biological applications as internal light sources in biological bodies upon irradiation from outside. In such applications, different kinds of photoreceptor molecules having optical absorption in different wavelength regions are used. To be used in a noninvasive manner, nanoparticles are appropriate. Also, to achieve high stopping power for external irradiation of, e.g., X-rays, high density and effective atomic number are desirable. In this study, to fulfill these requirements, we developed nanoparticle scintillators based on $Gd_3Al_3Ga_2O_{12}$ (GAGG). To achieve emission in the yellow-to-red wavelength region, we doped Pr^{3+} ions in GAGG. We successfully developed GAGG scintillator nanoparticles of less than 100 nm that exhibit photoluminescence (PL) and scintillation at the yellow-to-red wavelength region owing to the 4f–4f transitions of Pr^{3+} ions. The PL quantum yield of 62% was achieved at the Pr concentration of 1 mol%.

1. Introduction

Various kinds of phosphors have been used for radiation detection. Depending on the mode of radiation detection, different kinds of phosphors are used. In active-type radiation detectors, prompt luminescence of phosphors, i.e., scintillation, has been used. Scintillation occurs via various kinds of radiative electronic transitions and differs in different kinds of materials. For X-ray and gamma ray detection, the atomic numbers of the constituent elements and the density of the scintillator should be high, whereas ^{6}Li or ^{10}B should be contained at high concentrations for thermal neutron detection. Also, radiation tolerance, chemical stability, and cost are different for different kinds of scintillators. Hence, various types of compounds and their hybrids have been utilized to develop scintillators. Among inorganic scintillators,[1] single crystals,[2–14] transparent ceramics,[15,16] and glasses[17–20] of various compounds and compositions have been utilized in the development of novel scintillators. As scintillators based on organic materials,[21,22] organic liquid,[23–25] crystalline,[26,27] and plastic[28–35] ones have been developed. Moreover,

*Corresponding author: e-mail: koshimizu.masanori@shizuoka.ac.jp
https://doi.org/10.18494/SAM6015

ISSN 0914-4935
https://myukk.org/

organic–inorganic hybrid materials[36–51] have also been developed for scintillators. In contrast, in passive-type radiation detectors, an accumulated dose of ionizing radiation can be measured using storage-type phosphors exhibiting thermally stimulated luminescence,[52–57] optically stimulated luminescence,[52,53,58,59] and radiophotoluminescence.[60–65] Phosphors having the appropriate properties can be selected to be used in specific applications.

In addition to radiation detection, phosphors have been recently utilized in *in vivo* applications. Recent reports have shown that scintillators can be used in optogenetics technologies.[66,67] In such applications, scintillators are preferable because prompt emission of photons can be used in optogenetics. To obtain efficient emission upon external X-ray irradiation, high density and high effective atomic number are required for scintillators. In addition, scintillators of small sizes are preferable from the viewpoint of their noninvasive introduction. To fulfill these requirements, we have developed $Gd_3Al_3Ga_2O_{12}$ (GAGG)-based nanoparticle scintillators as they have high density, high effective atomic number, and high scintillation light yields. Among them, Ce-[68] and Eu-doped[69] ones have been developed to realize emission at different wavelength regions. In this study, we used Pr^{3+} as the luminescent centers to realize the scintillation in the yellow-to-red wavelength region.

2. Materials and Methods

The Pr-doped GAGG nanoparticles were synthesized according to the procedure in previous studies.[68,69] Distilled water (Wako), L(+)-tartaric acid (99.5%, Wako), $Gd(NO_3)_3 \cdot 6H_2O$ (99.99%, Sigma–Aldrich), $Al(NO_3)_3 \cdot 9H_2O$ (99.9%, Wako), $Ga(NO_3)_3 \cdot nH_2O$ (99.999%, Kojundo Chemical Laboratory), and $Pr(NO_3)_3 \cdot 6H_2O$ (99.9%, Sigma–Aldrich) were used without further purification. The hydration number n of $Ga(NO_3)_3 \cdot nH_2O$ was estimated by measuring the Ga concentration in an aqueous solution of $Ga(NO_3)_3 \cdot nH_2O$ using inductively coupled plasma optical emission spectroscopy (ICP-AES; Optima 2100DV, PerkinElmer). Stoichiometric ratios of $Gd(NO_3)_3 \cdot 6H_2O$, $Al(NO_3)_3 \cdot 9H_2O$, $Ga(NO_3)_3 \cdot nH_2O$, and $Pr(NO_3)_3 \cdot 6H_2O$ were dissolved in a 0.6 mol/L aqueous solution of tartaric acid. We synthesized samples with Pr concentrations up to 10 mol% with respect to (Gd+Pr). The total metal concentration was half that of tartaric acid. After the dissolution, the solution was stirred for 24 h at room temperature with an aluminum lid, stirred for 2 h at 80 °C, and dried at 80 °C after removing the lid for one night to obtain a dry gel. The dry gel was calcined at 1300 °C for 6 h to obtain the nanoparticles. In the rare-earth-doped garnet scintillators grown via melt growth, the composition of the crystal is often quite different from that of the raw materials. Contrary to the melt growth, the synthesis procedure in this study has no segregation process among the constituent elements. Hence, if the segregation does not spontaneously occur within the samples or a specific metal component does not volatilize from the samples, the samples have the same metal composition as that of the raw materials. According to our previous study on Ce-doped GAGG nanoparticles,[68] a reduction in the photoluminescence (PL) quantum yield (QY) was observed at 1400 °C, possibly owing to the volatilization of Ga. On the basis of these considerations, the metal compositions of the samples are judged to be the same as those of the raw materials. A photograph of samples with different

Pr concentrations is presented in Fig. 1. The powder became light green with increacing Pr concentration.

The X-ray diffraction (XRD) patterns of the samples were obtained using a diffractometer (RINT-2000, Rigaku) equipped with a Cu anode operated at 40 kV and 20 mA. The morphology of the samples was characterized using TEM (JEM-2100F, JEOL). The PL excitation and emission maps and PL QYs were obtained using a spectrofluorometer (C11347, Hamamatsu). The X-ray-induced radioluminescence (XRL) spectra were obtained using X-rays from an X-ray generator (XRB80N100 Monoblock, Spellman) operated at 80 kV and 1.2 mA as the excitation source and a CCD-based detector (DU920-BU2, Andor) equipped with a monochromator (Shamrock 163 Imaging Spectrograph, Andor) as the detector. Samples of similar quantities were attached to the tip of the optical fiber, which delivered the scintillation from the samples to the detector. The light collection efficiency may have varied with each measurement. Hence, only a qualitative comparison of the intensity is valid.

3. Results and Discussion

The XRD patterns of GAGG doped with Pr up to 10 mol% are presented in Fig. 2. A reference pattern of $Gd_3Al_2Ga_3O_{12}$[70] is also presented. The observed patterns are well consistent with the reference one, with no noticeable diffraction peaks of other crystalline phases. This result clearly indicates that the GAGG crystalline phase was successfully formed. The enlarged view at around 33° exhibits a negligible shift of the peak and a slight broadening with Pr concentration, which suggests a distribution of Pr concentration in the samples.

The TEM image of a GAGG nanoparticle doped with Pr at 0.1 mol% is presented in Fig. 3. We observed mostly ellipsoidal nanoparticles of less than 100 nm regardless of the Pr concentration. The size and the shape of the nanoparticles were similar to those of Ce-[68] and Eu-doped[69] GAGG nanoparticles.

The excitation–emission maps of the nanoparticles of GAGG doped with Pr at 0.1, 1, and 10 mol% are presented in Fig. 4. A broad emission band at 780 nm was observed with excitation at ~270 nm for all the samples. This band was also observed in nominally undoped GAGG.[69] A plausible origin of the band at around 780 nm may be Cr^{3+} ions. According to a previous report on Cr-doped GAGG,[71] the emission of the Cr^{3+} ions in GAGG was observed at 730 nm with

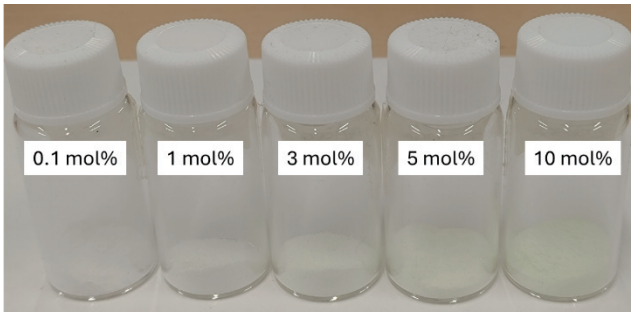

Fig. 1. (Color online) Photograph of samples.

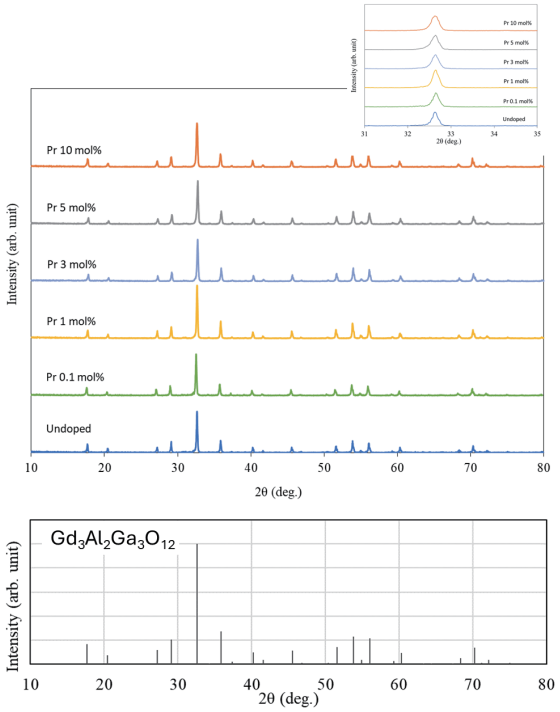

Fig. 2. (Color online) XRD patterns of nanoparticles of GAGG doped with Pr up to 10 mol% and a reference pattern of $Gd_3Al_2Ga_3O_{12}$.[70] The inset is an enlarged view around 33°.

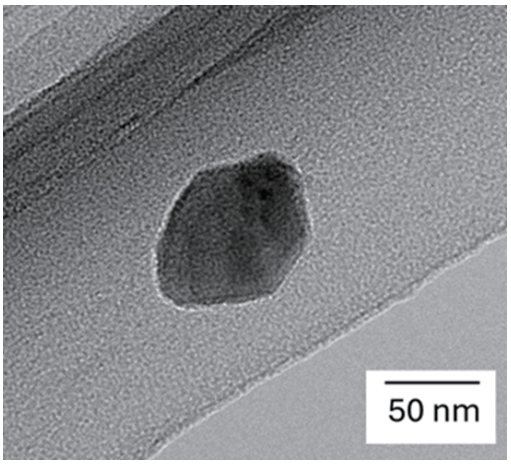

Fig. 3. TEM image of nanoparticle of GAGG doped with Pr at 0.1%.

excitation bands at 290, 445, and 625 nm. Hence, Cr^{3+} ions are excluded as the candidate origin. According to a recent report on Fe-doped $Y_3Al_5O_{12}$,[72] an emission band was observed at 784 nm and attributed to the $^4T_1(^4G)$-to-$^6A_1(^6S)$ transition of Fe^{3+} ions. The emission band has an excitation band at around 280 nm attributed to the charge transfer excitation from O^{2-} to Fe^{3+}. The emission and excitation wavelengths are similar to those of the 780 nm band in the excitation–emission maps. Hence, the emission at around 780 nm is attributed to Fe^{3+} ions included as impurity. Sharp emission peaks were observed at around 490, 534, 603, 632, 662,

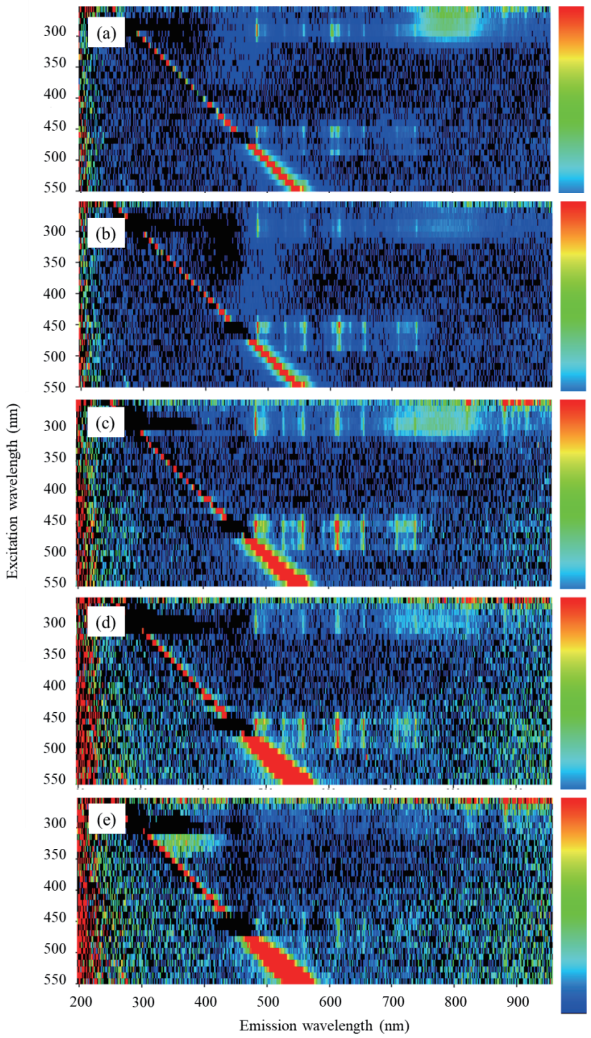

Fig. 4. (Color online) Excitation-emission maps of GAGG nanoparticles doped with Pr at (a) 0.1, (b) 1, (c) 3, (d) 5, and (e) 10 mol%.

and 727 nm: the peaks were more pronounced at low Pr concentrations. They are attributed to the 4f–4f electronic transitions of $^3P_0 \rightarrow {}^3H_4$, $^3P_0 \rightarrow {}^3H_5$, $^1D_2 \rightarrow {}^3H_4$, $^3P_0 \rightarrow {}^3H_6$, $^3P_0 \rightarrow {}^3F_2$, and $^3P_0 \rightarrow {}^3F_4$ of Pr^{3+}, respectively.[73] Excitation bands for these emission bands were observed at around 280 nm and 440–500 nm, and are attributed to the 4f–5d transition and the 4f–4f transition from $^3H_4$ to $^3P_0$, $^3P_1$, and $^3P_2$ states of Pr^{3+}, respectively.[73] A broad emission band at 300–400 nm was observed for the sample with a Pr concentration of 10 mol% and is attributed to the 5d–4f transition of Pr^{3+} ions.[74] The PL QYs of the samples with different Pr concentrations are summarized in Table 1. The highest PL QY of 62% was achieved at the Pr concentration of 1 mol%. The low PL QY at the Pr concentration of 0.1 mol% may be attributed to the absorption of the excitation light by the Fe impurities. The low PL QYs at high Pr concentrations are attributed to the concentration quenching. The decrease in the PL QY from the Pr concentration of 1 mol% to 10 mol% was not straightforward; unfortunately, the reason for this dependence is unclear at present.

Table 1
PL QY of samples with different Pr concentrations.

Pr concentration (mol%)	0.1	1	3	5	10
PL QY (%)	50	62	17	29	9

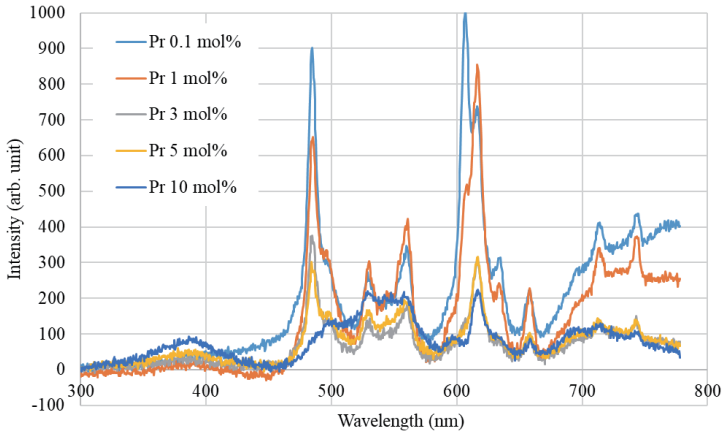

Fig. 5. (Color online) XRL spectra of GAGG nanoparticles doped with Pr at different concentrations.

The XRL spectra of the nanoparticles of GAGG doped with Pr at different concentrations are presented in Fig. 5. The light collection efficiency may have varied with each measurement. Hence, the intensity was normalized to its maximum in each spectrum. The XRL spectra were composed of the emission bands that were also observed in the PL spectra. The spectra of the nanoparticles of GAGG doped with Pr at 0.1 and 1 mol% were similar. The spectrum of the nanoparticles of GAGG doped with Pr at 10 mol% was different in three spectral regions: the first one is at around 780 nm, where the broad band emission, possibly owing to the Fe impurities, is located. The relative intensity of this band is significantly reduced at the Pr concentration of 10 mol%, which is because the energy transfer efficiency to the Fe impurity sites was reduced at a high Pr concentration owing to the competition of the energy transfer to Fe and Pr sites. The second one is the high relative intensity of the emission bands at 500–600 nm, which is possibly related to the slight change in the symmetry of the crystal field of the site of the Pr^{3+} ions. The third one is the enhanced relative intensity of the 5d–4f transition at 300–420 nm, which is consistent with the PL spectra presented in Fig. 4. To obtain the emission in the yellow-to-red region, low Pr concentrations are appropriate.

4. Conclusions

We developed nanoparticles of GAGG doped with Pr at different concentrations to obtain the yellow-to-red emission from Pr^{3+} ions. We successfully fabricated nanoparticles with the GAGG crystalline structure without alien phases and having sizes less than 100 nm. We observed many emission bands at 490–800 nm, most of which are attributed to the 4f–4f transitions of Pr^{3+} ions. We also observed emission at 300–400 nm owing to the 5d–4f transition of Pr^{3+} ions at high Pr

concentrations. A similar emission was also observed in the XRL spectra. The highest PL QY of 62% was achieved at the Pr concentration of 1 mol%.

Acknowledgments

This research was supported by a Grant-in-Aid for Scientific Research (A) (22H00308, 2022–2025). A part of this research is based on the Cooperative Research Project of the Research Center for Biomedical Engineering, Ministry of Education, Culture, Sports, Science and Technology of Japan.

References

1 T. Yanagida, T. Kato, D. Nakauchi, and N. Kawaguchi: Jpn. J. Appl. Phys. **62** (2023) 010508.
2 D. Nakauchi, T. Kato, N. Kawaguchi, and T. Yanagida: Sens. Mater. **37** (2025) 547.
3 K. Ichiba, K. Watanabe, K. Okazaki, T. Kato, D. Nakauchi, N. Kawaguchi, and T. Yanagida: Sens. Mater. **37** (2025) 553.
4 K. Okazaki, M. Koshimizu, D. Nakauchi, Y. Takebuchi, K. Ichiba, H. Ezawa, T. Kato, N. Kawaguchi, and T. Yanagida: Sens. Mater. **37** (2025) 557.
5 T. Kunikata, K. Okazaki, H. Kimura, S. Takase, T. Kato, D. Nakauchi, N. Kawaguchi, and T. Yanagida: Sens. Mater. **37** (2025) 563.
6 K. Miyazaki, D. Nakauchi, Y. Takebuchi, T. Kato, N. Kawaguchi, and T. Yanagida: Sens. Mater. **37** (2025) 587.
7 M. Ishida, A. Watanabe, H. Kawamoto, Y. Fujimoto, and K. Asai: Sens. Mater. **37** (2025) 607.
8 K. Ichiba, T. Kato, D. Nakauchi, N. Kawaguchi, and T. Yanagida: Sens. Mater. **36** (2024) 451.
9 T. Kunikata, P. Kantuptim, D. Shiratori, T. Kato, D. Nakauchi, N. Kawaguchi, and T. Yanagida: **36** (2024) 457.
10 Y. Endo, K. Ichiba, D. Nakauchi, T. Kato, N. Kawaguchi, and T. Yanagida: Sens. Mater. **36** (2024) 473.
11 H. Fukushima, D. Nakauchi, T. Kato, N. Kawaguchi, and T. Yanagida: Sens. Mater. **36** (2024) 489.
12 H. Kimura, H. Fukushima, K. Watanabe, T. Fujiwara, H. Kato, M. Tanaka, T. Kato, D. Nakauchi, N. Kawaguchi, and T. Yanagida: Sens. Mater. **36** (2024) 507.
13 K. Miyazaki, D. Nakauchi, T. Kato, N. Kawaguchi, and T. Yanagida: Sens. Mater. **36** (2024) 515.
14 K. Yamabayashi, K. Okazaki, D. Nakauchi, T. Kato, N. Kawaguchi, and T. Yanagida: Sens. Mater. **36** (2024) 523.
15 T. Kato, D. Nakauchi, N. Kawaguchi, and T. Yanagida: Sens. Mater. **36** (2024) 531.
16 T. Ubukata, S. Otake, T. Kato, D. Nakauchi, N. Kawaguchi, and T. Yanagida: J. Lumin. **278** (2025) 121021.
17 K. Miyajima, A. Nishikawa, T. Kato, D. Nakauchi, N. Kawaguchi, and T. Yanagida: Sens. Mater. **37** (2025) 481.
18 H. Fukushima, R. Tsubouchi, T. Matsuura, T. Yoneda, and T. Yanagida: Sens. Mater. **37** (2025) 487.
19 D. Nakauchi, H. Kimura, D. Shiratori, T. Kato, N. Kawaguchi, and T. Yanagida: Sens. Mater. **36** (2024) 573.
20 Y. Takebuchi, A. Masuno, D. Shiratori, K. Ichiba, A. Nishikawa, T. Kato, D. Nakauchi, N. Kawaguchi, and T. Yanagida: Sens. Mater. **36** (2024) 579.
21 M. Koshimizu: Jpn. J. Appl. Phys. **62** (2023) 010503.
22 M. Koshimizu: J. Lumin. **278** (2025) 121008.
23 S. Arai, M. Koshimizu, Y. Fujimoto, T. Yanagida, and K. Asai: Nucl. Instrum. Methods Phys. Res. A **954** (2020) 161632.
24 A. Watanabe, A. Magi, M. Koshimizu, A. Sato, Y. Fujimoto, and K. Asai: Sens. Mater. **33** (2021) 2251.
25 A. Watanabe, M. Koshimizu, K. Watanabe, A. Sato, Y. Fujimoto, and K. Asai: Phys. Chem. Chem. Phys. **26** (2024) 9329.
26 A. Sato, M. Koshimizu, Y. Fujimoto, S. Komatsuzaki, S. Kishimoto, and K. Asai: Mater. Chem. Front. **6** (2022) 1470.
27 V. Govindan, D. Joseph Daniel, H. J. Kim, and K. Sankaranarayanan: Mater. Chem. Phys. **223** (2019) 183.
28 M. Koshimizu, G.H.V. Bertrand, M. Hamel, S. Kishimoto, R. Haruki, F. Nishikido, T. Yanagida, Y. Fujimoto, and K. Asai: Jpn. J. Appl. Phys., **54** (2015) 102202.
29 M. Koshimizu, T. Yanagida, R. Kamishima, Y. Fujimoto, and K. Asai: Sens. Mater. **31** (2019) 1233.

30 K. Kagami, M. Koshimizu, Y. Fujimoto, S. Kishimoto, R. Haruki, F. Nishikido, and K. Asai: Radiat. Meas. **135** (2020) 106361.
31 A. Magi, M. Koshimizu, Y. Fujimoto, T. Yanagida, and K. Asai: Radiat. Meas. **137** (2020) 106401.
32 A. Sato, A. Magi, M. Koshimizu, Y. Fujimoto, S. Kishimoto, and K. Asai: RSC Adv. **11** (2021) 15581.
33 A. Sato, M. Koshimizu, Y. Fujimoto, and K. Asai: Opt. Mater. **136** (2023) 113493.
34 N. Hayashi and M. Koshimizu: J. Lumin. **277** (2025) 120993.
35 N. Hayashi and M. Koshimizu: Jpn. J. Appl. Phys. **64** (2025) 10SP06.
36 M. Koshimizu: Funct. Mater. Lett. **13** (2020) 2030003.
37 S. Takigawa, M. Koshimizu, T. Noguchi, T. Aida, S. Takami, T. Adschiri, Y. Fujimoto, A. Yoko, G. Seong, T. Tomai, and K. Asai: J. Radioanal. Nucl. Chem. **314** (2017) 611.
38 S. Arai, T. Noguchi, T. Aida, A. Yoko, T. Tomai, T. Adschiri, M. Koshimizu, T. Fujimoto, and K. Asai: J. Ceram. Soc. Jpn. **128** (2019) 28.
39 A. Watanabe, A. Magi, A. Yoko, G. Seong, T. Tomai, T. Adschiri, Y. Hayashi, M. Koshimizu, Y. Fujimoto, and K. Asai: Nanomaterials **11** (2021) 1124.
40 Y. Araya, M. Koshimizu, R. Haruki, F. Nishikido, S. Kishimoto, and K Asai: Sens. Mater. **27** (2015) 255.
41 F. Hiyama, T. Noguchi, M. Koshimizu, S. Kishimoto, R. Haruki, F. Nishikido, T. Yanagida, Y. Fujimoto, T. Aida, S. Takami, T. Adschiri, and K. Asai: Jpn. J. Appl. Phys. **57** (2018) 012601.
42 F. Hiyama, T. Noguchi, M. Koshimizu, S. Kishimoto, R. Haruki, F. Nishikido, Y. Fujimoto, T. Aida, S. Takami, T. Adschiri, and K. Asai: Jpn. J. Appl. Phys. **57** (2018) 052203.
43 K. Inoue, M. Koshimizu, F. Hiyama, K. Asai, F. Nishikido, R. Haruki, and S. Kishimoto: IEEE Trans. Nucl. Sci. **65** (2018) 1012.
44 K. Kagami, M. Koshimizu, Y. Fujimoto, S. Kishimoto, R. Haruki, F. Nishikido, and K. Asai: J. Mater. Sci. Mater. Electron. **31** (2020) 896.
45 S. Kishimoto, M. Koshimizu, F. Hiyama, R. Haruki, and F. Nishikido: Nucl. Instrum. Methods Phys. Res. A **968** (2020) 163908.
46 A. Magi, M. Koshimizu, A. Watanabe, A. Yoko, G. Seong, T. Tomai, T. Adschiri, R. Haruki, F. Nishikido, S. Kishimoto, Y. Fujimoto, and K. Asai: J. Mater. Sci. Electron. **32** (2021) 7987.
47 A. Magi, M. Koshimizu, A. Sato, Y. Fujimoto, S. Kishimoto, T. Yanagida, and K. Asai: Jpn. J. Appl. Phys. **62** (2022) SB1036.
48 A. Sato, M. Koshimizu, Y. Fujimoto, S. Kishimoto, and K. Asai: J. Mater. Sci. Electron. **32** (2021) 28807.
49 A. Sato, Y. Fujimoto, K. Asai, and M. Koshimizu: Jpn. J. Appl. Phys. **63** (2024) 01SP06.
50 H. Tsukahara, Y. Fujimoto, K. Asai, and M. Koshimizu: J. Lumin. **271** (2024) 120592.
51 H. Tsukahara and M. Koshimizu: J. Mater. Sci. Electron. **36** (2025) 1223.
52 H. Ezawa, Y. Takebuchi, K. Okazaki, T. Kato, D. Nakauchi, N. Kawaguchi, and T. Yanagida: Sens. Mater. **36** (2024) 465.
53 H. Kimura, T. Fujiwara, H. Kato, M. Koshimizu, G. Wakabayashi, Y. Takebuchi, T. Kato, D. Nakauchi, N. Kawaguchi, and T. Yanagida: Sens. Mater. **37** (2025) 599.
54 M. Koshimizu, K. Oba, Y. Fujimoto, and K. Asai: Sens. Mater. **36** (2024) 565.
55 H. Fujiwara, T. Negishi, L. Takahashi, and K. Shinsho: Sens. Mater. **37** (2025) 463.
56 T. Kato, A. Nishikawa, D. Nakauchi, N. Kawaguchi, and T. Yanagida: Sens. Mater. **37** (2025) 475.
57 H. Yamaguchi, M. Koshimizu, H. Kawamoto, Y. Fujimoto, G. Wakabayashi, and K. Asai: Radiat. Phys. Chem. **220** (2024) 111703.
58 S. Otake, H. Sakaguchi, Y. Yoshikawa, T. Kato, D. Nakauchi, N. Kawaguchi, and T. Yanagida: Sens. Mater. **36** (2024) 539.
59 Y. Takebuchi, M. Morioka, Y. Nakashima, K. Tezuka, H. Kimura, S. Otake, and T. Yanagida: Sens. Mater. **37** (2025) 525.
60 M. Koshimizu: Radiat. Meas. **176** (2024) 107222.
61 A. Nishikawa, D. Shiratori, T. Kato, D. Nakauchi, N. Kawaguchi, and T. Yanagida: Sens. Mater. **36** (2024) 597.
62 H. Kawamoto, Y. Fujimoto, and K. Asai: Sens. Mater. **36** (2024) 607.
63 R. Tanaka, M. Koshimizu, I. Kawamura, Y. Fujimoto, and K. Asai: J. Mater. Sci. Electron. **33** (2022) 3938.
64 R. Tanaka, M. Koshimizu, Y. Fujimoto, and K. Asai: J. Lumin. **264** (2023) 120166.
65 R. Tanaka, M. Koshimizu, A. Watanabe, Y. Fujimoto, H. Kawamoto, and K. Asai: J. Lumin. **267** (2024) 120367.
66 T. Matsubara, T. Yanagida, N. Kawaguchi, T. Nakano, J. Yoshimoto, M. Sezaki, H. Takizawa, S. P. Tsunoda, S.-L. Horigane, S. Ueda, S. Takemoto-Kimura, H. Kandori, A. Yamanaka, and T. Yamashita: Nat. Commun. **12** (2021) 4478.

67 M. Hildebrandt, M. Koshimizu, Y. Asada, K. Fukumitsu, M. Ohkuma, N. Sang, T. Nakano, T. Kunikata, K. Okazaki, L. Lian, J. Zhang, T. Yanagida, and T. Yamashita: Int. J. Mol. Sci. **25** (2024) 11365.
68 M. Koshimizu, Y. Fujimoto, and K. Asai: Sens. Mater. **35** (2023) 521.
69 M. Koshimizu, K. Tanahashi, Y. Fujimoto, and K. Asai: Sens. Mater. **37** (2025) 539.
70 A. C. S. Hamilton, G. I. Lampronti, S. E. Rowley, and S. E. Dutton: J. Phys.: Condens. Matter **26** (2014) 116001.
71 H. Jiang, L. Chen, G. Zheng, Z. Luo, X. Wu, Z. Liu, R. Li, Y. Liu, P. Sun, J. Jiang: Adv. Opt. Mater. **10** (2022) 2102741.
72 R. Zhaoa, X. Guoa, J. Zhangb, and R. Cui: J. Lumin. **267** (2024) 120352.
73 J. P. Zuniga, S. K. Gupta, M. Pokhrel, and Y. Mao: New J. Chem. **42** (2018) 9381.
74 K. Kamada, T. Yanagida, J. Pejchal, M. Nikl, T. Endo, K. Tsutumi, Y. Usuki, Y. Fujimoto, A. Fukabori, and A. Yoshikawa: J. Cryst. Growth **352** (2012) 84.